Steady-State Luminescence of Polymers

Ramon Reigada†

Facultat de Química, Universitat de Barcelona, C/Martí i Franquès 1, 08028 Barcelona, Spain

Igor M. Sokolov*

Institut für Physik, Humboldt-Universität zu Berlin, Newtonstr. 15, D-12489 Berlin, Germany

Received July 12, 2004; Revised Manuscript Received January 6, 2005

ABSTRACT: We consider a simple model for steady-state luminescence of single polymer chains in a dilute solution in the case when excitation quenching is due to energy transfer between a donor and an acceptor attached to the ends of the chain. We present numerical results for Rouse chains without or with hydrodynamic interactions, which are taken into account in a perturbative manner. We consider the situations of a quiescent solvent as well as the chain in a shear flow and discuss the dependence of the steady-state luminescence intensity on the strength of hydrodynamic interaction and on the shear rate in the flow.

1. Introduction

The kinetics of reactions where polymers are involved has attracted much attention in the last 2 decades due to its experimental relevance and to a large variety of applications. In particular, luminescent energy transfer in polymers is an important phenomenon (see, e.g., ref 1). Luminescent markers are used for probing both the intrinsic polymer dynamics and the properties of their solvent environment. However, such dynamical phenomena definitely belong to the most complex problems in diffusion−reaction processes, and no satisfactory theoretical approaches have been found to provide a reasonable description. The problem relies on the complicated nonmarkovian dynamics of the system, where the most interesting phenomena take place on the time scales on which the systems show strong memory effects. Even the corresponding initial condition problem is hard to solve, and no satisfactory quantitative theory exists at present for the stationary case.

Let us start from formulating the problem, and discuss the simplest energy transfer model, which will be used throughout the article. Let us assume that the ends of a polymer are marked (e.g., by a donor monomer and an acceptor monomer). The molecule is under constant irradiation at a resonant probe frequency, so that the donor can get excited with probability λ per unit time (we consider λ as the effective intensity of the irradiation). The relaxation of the excited state due to spontaneous emission, as well as nonlinear effects connected with possible multiple excitation are neglected, so that the only mechanism of relaxation is the donor−acceptor energy transfer. We assume that the corresponding energy transfer is accompanied by emission of a photon with a frequency different to that one of the applied irradiation. In a typical situation, taking place in fluorescence resonance energy transfer (FRET), the efficiency of energy transfer is dependent on the inverse sixth power of the donor−acceptor separation. This dependence is so steep that one typically introduces a reaction radius a and assumes the lifetime of the excited-state being infinite when the distance between donor and acceptor is larger than a and practically zero if this distance is smaller than a. This is exactly the model we use throughout the present article.

The overall situation is depicted in Figure 1, where a short part of the simulated time dependence of the end-to-end distance, $r(t)$, is shown for a simple Rouse chain of length $N = 21$ in a quiescent solvent, vide infra. The bar-code-like set of rectangles shown in gray in the lower part of the picture shows the times, when $r(t) < a$ (at rather low resolution). The typical FRET situation corresponds to the case when the absorption of a photon at time t_1, when $r(t) < a$ is immediately followed by photon emission. For $r(t) > a$, the absorption of the photon at time t_2 excites the system, which stays in an excited state until $r(t)$ reaches again the reaction radius a, and then the emission follows. We shall say that for $r(t) < a$ the donor−acceptor system is in its *off*-state and when $r(t) > a$ it is in its *on*-state. This notation corresponds to the ability of a donor to keep its excited state for a considerable time. In what follows, the expressions *on* and *off* will be simply used for denoting states in which the end-to-end distance is above and below the reaction radius a, respectively. Now, the probability that a photon arrives when the system is in the *off*-state is proportional to the probability to find the end-to-end distance $r(t) < a$, which can be immediately calculated from the equilibrium (or, in the case of polymers in flows, steady-state) end-to-end distance distribution. Moreover, the intensity of the fluorescence in the *off*-state is then proportional to the intensity of irradiation, since the probability of excitation being in the *off*-state is constant. On the other hand, the excitation in the *on*-state is not immediately followed by the emission of a photon. This is an essentially nonequilibrium phenomenon, probing the *dynamics* of the end-to-end changes. As we proceed to show, the dependence of the intensity of this process on the intensity of irradiation is nonlinear, so that it can be distinguished from the equilibrium background. When thinking about experimental realizations of the process, one must take into account that even if FRET does not take place, the lifetime of the excited state of the donor if finite. This means that for very long molecules, whose

* Corresponding author. E-mail: igor.sokolov@physik.hu-berlin.de.

† E-mail: reigada@ub.edu.

10.1021/ma048593b CCC: $30.25
Published on Web 03/17/2005

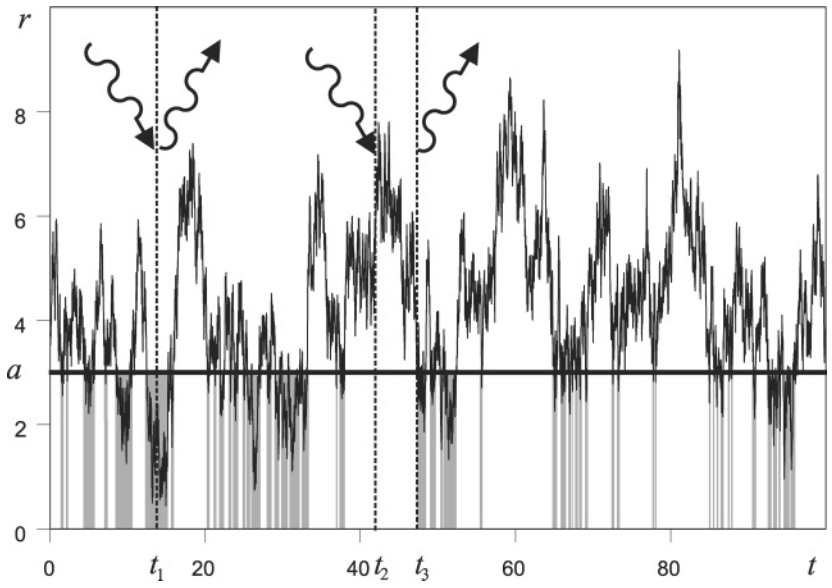

Figure 1. A short part of the trajectory $r(t)$ for a Rouse chain and explanation of the definition of the *on*-state ($r > a$, here $a = 3$) and the *off*-state ($r < a$) of the system. See text for details. In a typical FRET situation, the photon absorption occurring in the *off*-state (for example at $t = t_1$), is immediately followed by photon emission. If the absorption takes place in the *on*-state (for example at $t = t_2$), the photon is emitted when entering the *off*-state (at $t = t_3$). The bar-code-like set of gray rectangles denotes the times the system spends in its *off*-state.

Rouse time is compared to this lifetime or longer, this nonlinear component is weakened. For such long molecules, one can consider marking the ends by a monomer which has a triplet excited state (having a very long lifetime) and by a corresponding quencher. However, the reaction radii in this case are very small.

For modeling purposes, we first consider the following hypothetical situation which emphasizes the *crossing* from one state to another. We fully disregard the emission in the *off*-state and take for the time being that being close to the acceptor ($r(t) < a$), the donor cannot be excited. In this case, being in the *on*-state, the system may be excited with probability λ per unit time and emits the photon with the observation frequency under the transition into the *off*-state, whereas in the *off*-state the system cannot be excited; i.e., it is simply "off". Our *on*−*off* model does not closely model the FRET situation, where the donor−acceptor interactions are typically too small to bring the system out of resonance. However, it still can be a reasonable approximation in the case when the reaction radii are small. Moreover, the results for the realistic situation can be obtained from the ones for the *on*−*off*-model by adding a term linear in λ, vide infra.

The overall situation might seem simple; however, it is much more complicated than the case of irreversible cyclization[2−8] and extremely awkward for theoretical investigation, even in the absence of flow. Our knowledge about the reaction kinetics under flow is sporadic even for simpler reactions (see, e.g., refs 9 and 10).

The whole problem would be easily solvable if the lifetime distributions in the *on*- and the *off*-states were known. Then the probability for it to be excited being in the *on*-state and therefore the intensity of the emitted light could be easily calculated. The probabilities to be in either state are connected with the level-crossing properties of the random process $r(t)$. As for all diffusive processes, however, the level-crossing process by $r(t)$ shows a fractal structure (corresponding to the fractal structure of the bar-code-set in Figure 1), so that the meantime between two such crossings is zero. This follows immediately from the Rice formula for level crossing density[11] and from the form of the two-time correlation function of the end-to-end distances, e.g., for a Rouse polymer, which function lacks the second derivative at zero. Again, as for all diffusive processes, this leads to a "tremor" in which $r(t)$ crosses the a-level many times until it leaves and performs a long excursion to either side. This "tremor" is due to the fact that the diffusion approximation (Wiener process) used in the description of the chain (for example through the Rouse-like Langevin dynamics) does not adequately mirror the short-time dynamics of whatever physical system is used.[12] However, the existence of this theoretical problem does to no extent require any change of the model (e.g., by introducing underdamped dynamics, as proposed in ref 12) since the physical problem at hand does not depend on the too-small time behavior of the $r(t)$-process. Indeed, this process is randomly sampled at times t_i given by a Poissonian flow of photons following the rate λ. The behavior of $r(t)$ at times much smaller than λ^{-1} thus cannot be sampled and can physically play no role: this statement is a close analogue of Nyquist's sampling theorem. Thus, the absence of the lifetime distributions is not a problem of our theoretical model, but a problem of standard mathematical tools which rely too much on the unphysical, but absolutely unimportant, short-time properties of a Wiener process.

Therefore, in what follows, we concentrate on the numerical investigation of the proposed model and consider the intensity of stationary luminescence of the polymer $I(\lambda)$ under constant irradiation. We discuss the Rouse model without hydrodynamic interactions, as well as the role of hydrodynamic interactions between the monomers treated in a perturbative manner. Although such an approach is limited to weak hydrodynamic interaction (the effective hydrodynamic radii of monomers are small compared to the typical distances between them), the trends obtained here from the numerical simulations will definitely persist at realistic interaction strengths. We also consider the case when the polymer molecule undergoes deformation in a shear

flow, which does not however cause the full stretching of the molecule. This situation is especially interesting as the case when the stationary luminescence of diluted polymer solution can be used as a probe for the flow structure. The authors are not aware of any experimental work using this kind of measurement; thus our numerical study might serve as a proof-of-principle for such immediate flow diagnostics method.

2. Simulation Approach

Let us start by discussing the numerical procedure used in this paper. It consists of two independent parts: first, the simulation of the $r(t)$-trajectories, which are stored with high enough resolution, and second, their analysis, giving the steady-state luminescence intensity $I(\lambda)$. The reason for this approach is that one realization of the process can then be used to obtain $I(\lambda)$ for a variety of parameters a and λ of the model, so that the most time-consuming part of the simulation is done only once for the time necessary to get enough statistics. The time resolution of stored data has to be much smaller than the minimal λ^{-1} used to calculate $I(\lambda)$.

Let us concentrate first on the last part of the problem, namely on the evaluation of the stationary luminescence intensity for a given realization of the $r(t)$-process. From the record of the $r(t)$ we define the a-crossings of the process and, for given a, obtain the lengths of *on*- and *off*-intervals, which are ordered and stored. According to the Poisson statistics, the probability of not getting excited during a given *on*-interval of duration t_{on} is exactly $\exp(-\lambda t_{on})$. Thus, the probability of emitting light after the *on*-excursion is equal to $1 - \exp(-\lambda t_{on})$. Since the total intensity of emitted light for one polymer is proportional to the overall number of the intervals during which the system made a transition into its excited state, we have for the model where the *off*-state is not excitable:

$$I(\lambda) = \frac{1}{T}\sum_{i=1}^{n(a,T)} [1 - \exp(-\lambda t_i)] \tag{1}$$

where i numbers the *on*-intervals, $n(a, T)$ is their overall number, which depends on the reaction radius a and on the overall time of simulations T. For an ensemble of polymers in solution with the individual behavior described above, the steady intensity of emitted light in the *on*−*off* model is expected to be proportional to expression 1. Accordingly, the steady-state luminescence of an irradiated polymer solution should show, in practice, a relation between the intensities of the emitted light and the incident irradiation in agreement with the numerical estimation of eq 1 for our chain model (see below). In this work, we numerically study the modification of such dependence by the effect of a flow, and we suggest that this observation can be used as a flow detection method in experiments with polymer solutions.

Equation 1 shows that the intervals of very small duration are sampled with the probability proportional to their lengths so that, as anticipated, the fractal structures in vicinity of the concentration points of the level-crossings are not resolved and play no role. Using eq 1 it is possible to scan the whole range of intensities λ within one run, which is necessary to detect nonlinear effects. The situation in which, being in the *off*-state, the molecule immediately emits light, corresponds to the case when, being in the *off*-state the molecule can get excited whenever a photon arrives. Assuming the photons to arrive in a Poissonian manner, we get that the intensity in the *off*-state is simply proportional to the probability of being in this state, so that the overall intensity follows by adding this one to the expression given by eq 1

$$I_1(\lambda) = I(\lambda) + \lambda P_{off} \tag{2}$$

where P_{off} is the probability to be in the *off*-state, i.e., the overall relative time spent by the ends of a Gaussian chain within a sphere of radius a. Since this simply corresponds to adding a linear function of λ to the results for the *on*−*off* model, we concentrate in what follows only on these results, given by eq 1. However, a few words on the calculation of P_{off} are in order.

Since the distribution of the end-to-end distance for such a chain as a Gaussian, the corresponding probability can easily be calculated:

$$P_{off} = \int_{\Omega(a)} p(\mathbf{r})\, d\mathbf{r} \tag{3}$$

where $p(\mathbf{r})$ is the distribution of the end-to-end distances and the integration region $\Omega(a)$ corresponds to the reaction sphere of radius a. The case without flow, due to the spherical symmetry of $p(\mathbf{r})$, is especially simple. Since $p(\mathbf{r})$ in this case is a function of only the absolute value of the distance r, P_{off} depends only on the relative reaction radius $\rho = a/\sqrt{\langle L^2\rangle}$, where $\langle L^2\rangle$ is the mean end-to-end squared distance for the chain. The integration gives

$$P_{off}(\rho) = \mathrm{erf}\left(\sqrt{\frac{3}{2}}\rho\right) - \rho\sqrt{\frac{6}{\pi}}\exp\left(-\frac{3}{2}\rho^2\right) \tag{4}$$

with $\mathrm{erf}(x)$ being the error function. This result holds for all situations without flow.

For the case with flow, the end-to-end distribution loses its spherical symmetry, and leads to more complicated expressions. In the situation with flow and with hydrodynamic interactions, it is hard to get the analytical expression for P_{off}. We evaluate the corresponding probability from the numerical simulations, since it is simply proportional to the overall time spent in the *off*-state. The numerical results following from our simulations are presented in Tables 3 and 4.

Let us now turn to the first step of the proposed numerical procedure, which corresponds to the simulation of the trajectories.

2.1. The Rouse Model. We start from the Rouse chain as the simplest model for a polymer,[13,14] where

Table 1. Quality of Perturbative Approximations for $N = 21$

		$\langle E_{tot}\rangle$	$\langle L^2\rangle$
theoretical		30	20
Rouse simulation		30.185	21.028
Zimm, $r_0 = 0.1$	0-order	29.591	27.406
	1-order	30.763	21.020
	2-order	30.221	20.181
Zimm, $r_0 = 0.2$	0-order	31.190	36.923
	1-order	33.114	23.843
	2-order	31.676	21.839
Zimm, $r_0 = 0.5$	0-order	42.058	73.349
	1-order	49.344	44.741
	2-order	53.215	46.732

Table 2. Quality of Perturbative Approximations for $N = 51$

$N = 51$		$\langle E_{tot}\rangle$	$\langle L^2\rangle$
theoretical		75	50
Rouse simulation		75.323	48.122
Zimm, $r_0 = 0.1$	0-order	76.063	86.674
	1-order	77.412	54.021
	2-order	75.926	47.746
Zimm, $r_0 = 0.2$	0-order	81.399	130.64
	1-order	83.903	67.487
	2-order	79.167	51.600

Table 3. P_{off} for the Chain with $N = 21$

$\alpha = 0$	$a = 1$	$a = 4$	$a = 8$
$r_0 = 0$	0.014843	0.502626	0.974239
$r_0 = 0.05$	0.014831	0.499207	0.972863
$r_0 = 0.1$	0.013845	0.484438	0.969214
$\alpha = 0.0125$	$a = 1$	$a = 4$	$a = 8$
$r_0 = 0$	0.014 67	0.499 77	0.973 02
$r_0 = 0.05$	0.014 81	0.497 75	0.971 91
$r_0 = 0.1$	0.013724	0.482 83	0.968 35
$\alpha = 0.078$	$a = 1$	$a = 4$	$a = 8$
$r_0 = 0$	0.013605	0.443851	0.937554
$r_0 = 0.05$	0.013742	0.456638	0.947050
$r_0 = 0.1$	0.012997	0.450992	0.949065
$\alpha = 0.488$	$a = 1$	$a = 4$	$a = 8$
$r_0 = 0$	0.006830	0.156 18	0.438 74
$r_0 = 0.05$	0.007423	0.185 20	0.526 06
$r_0 = 0.1$	0.008600	0.209 18	0.589 51

Table 4. P_{off} for the Chain with $N = 51$

$\alpha = 0$	$a = 2$	$a = 7$	$a = 12$
$r_0 = 0$	0.034207	0.613049	0.960062
$r_0 = 0.05$	0.033190	0.594208	0.957482
$r_0 = 0.1$	0.028929	0.556314	0.945990
$\alpha = 0.002$	$a = 2$	$a = 7$	$a = 12$
$r_0 = 0$	0.033 86	0.614 18	0.959 83
$r_0 = 0.05$	0.032 70	0.594 12	0.957 56
$r_0 = 0.1$	0.029 32	0.556 41	0.946 33
$\alpha = 0.0125$	$a = 2$	$a = 7$	$a = 12$
$r_0 = 0$	0.033417	0.575235	0.933795
$r_0 = 0.05$	0.030730	0.571878	0.945019
$r_0 = 0.1$	0.027587	0.540211	0.939310
$\alpha = 0.078$	$a = 2$	$a = 7$	$a = 12$
$r_0 = 0$	0.016 09	0.201 26	0.459 65
$r_0 = 0.05$	0.024 17	0.282 67	0.615 73
$r_0 = 0.1$	0.012 73	0.308 60	0.676 50

the excluded volume effects and the hydrodynamical interactions between monomers are neglected. A Rouse chain is a set of N beads; each one, except for the two end beads, is connected to two neighbors by a harmonic potential, so that the overall potential energy of the system reads

$$V = \sum_{i=1}^{N-1} \frac{1}{2} k |\vec{r}_i - \vec{r}_{i+1}|^2 \tag{5}$$

where k is the harmonic spring constant and $\vec{r}_i$ corresponds to the position of the ith bead. The end beads are connected only to one neighbor. The coupled equations of motion of the chain correspond to an overdamped motion under the influence of thermal fluctuations:

$$\dot{r}_i = -\frac{1}{\gamma}\frac{\partial V}{\partial \vec{r}_i} + \frac{1}{\gamma}\vec{\eta}_i, \tag{6}$$

where γ is the friction parameter, and $\vec{\eta}_i$ is a zero-mean white noise obeying the fluctuation−dissipation relation,

$$\langle \eta_i^\alpha(t)\eta_j^\beta(t')\rangle = 2k_B T\gamma\delta_{ij}\delta_{\alpha\beta}\delta(t - t'). \tag{7}$$

In thermal equilibrium, the following relations following immediately from the canonical distribution have to hold independently on the model:

$$\langle E_{tot}\rangle = \frac{3}{2}(N - 1)k_B T \tag{8}$$

$$\langle d^2\rangle = \frac{3k_B T}{k} \tag{9}$$

$$\langle L^2\rangle = \frac{3(N - 1)k_B T}{k} \tag{10}$$

where E_{tot} is the total energy, and d and L stand for the bead-to-bead and end-to-end distances, respectively. These relations are always checked numerically as a proof of the quality of the simulation.

We also now apply a shear flow to the system, $\vec{v} = (\alpha y, 0, 0)$. The shear flow is implemented in eq 6 by including a term $+ \alpha y_i$ for the motion in the x-coordinate of each bead i

$$\dot{r}_i = -\frac{1}{\gamma}\frac{\partial V}{\partial \vec{r}_i} + \frac{1}{\gamma}\vec{\eta}_i + (\alpha y_i, \vec{0}, 0) \tag{11}$$

The characteristic intensity of the flow necessary to compare its effects on the chain's conformation in different situations is given by the value of the dimensionless parameter $\alpha\tau_R$ (Weissenberg number), with τ_R being the Rouse time.[8]

2.2. Hydrodynamic Interactions. The situation under hydrodynamic interactions is much more involved. The standard approaches[15−17] are very accurate but slow, so that we prefer an approximate perturbative one. The quality of the corresponding approximations is checked by calculating two thermodynamically fixed parameters of the chain in quiescent solvent: its mean end-to-end distance and the overall energy. In particular, the end-to-end distance in the chain was found to be extremely sensitive to improper incorporation of the hydrodynamic interaction. We confined ourselves to the situations under which the first and second order of the perturbation theory was found sufficient, as is the case up to hydrodynamic radii of the order of $^1/_5$ of the typical distance between the monomers. This is considerably smaller than the realistic value of around $^1/_2$. The slow convergence of perturbation series makes the use of such an approach unreasonable for larger radii. Therefore, in the present work, we only discuss some qualitative features, which can be seen when switching on the weak interaction and assume that they persist also when the interaction gets stronger.

The hydrodynamic interactions among the beads are modeled within the Zimm scheme.[18] The Zimm model is based on the Rouse chain model but the equations of motion for different beads are coupled to each other not only through elastic forces but also through hydrodynamic forces. Such coupling is a long-range one and is

introduced through the Oseen tensor,[19] which is a 3 × 3 tensor defined for each pair of beads $(i - j)$

$$\mathscr{H}_{ij} = \frac{1}{8\pi\eta|\vec{r}_{ij}|}[\vec{r}'_{ij}(\vec{r}'_{ij})^T + \mathscr{I}] \tag{12}$$

$$\mathscr{H}_{ii} = \frac{1}{\gamma}\mathscr{I} \tag{13}$$

where $\mathscr{I}$ is a unit matrix, $\vec{r}'_{ij}$ is a unit vector $\vec{r}_{ij}/|\vec{r}_{ij}|$ in the direction of $\vec{r}_{ij}$ and $(\vec{r}'_{ij})^T$ is its transpose. The viscosity parameter η can be expressed through γ and the bead's size r_0 since for $i = j$ one has $^1/_6\pi\eta r_0 = 1/\gamma$. Then,

$$\mathscr{H}_{ij} = \frac{3r_0}{4\gamma|\vec{r}_{ij}|}[\vec{r}'_{ij}(\vec{r}'_{ij})^T + \mathscr{I}] \tag{14}$$

In what follows we use $\gamma = 1$, which fixes the time scale of the presented numerical results. The equation of motion for the ith bead thus reads

$$\dot{r}_i = \sum_{j=1}^{N} \mathscr{H}_{ij}\left(\frac{\partial V}{\partial \vec{r}_j} + \vec{\eta}_j\right). \tag{15}$$

The noises $\vec{\eta}_j$ acting on different beads are now not independent; otherwise, the fluctuation−dissipation theorem would be violated. One often writes the corresponding equation of motion in the form

$$\dot{r}_i = \mathscr{H}\vec{f}_i + \sqrt{2k_BT}\mathscr{A}\vec{\psi} \tag{16}$$

where $\mathscr{H}$ is the $3N \times 3N$ matrix with the diagonal elements being unity (in the units where $\gamma = 1$) and with the nondiagonal elements denoting the Oseen terms between the corresponding components of velocity of different beads, and the matrix $\mathscr{A} = \sqrt{\mathscr{H}}$ is defined through $\mathscr{A}\cdot\mathscr{A}^T = \mathscr{H}$. The elements of the vector $\vec{\psi}$ are now independent, zero mean Gaussian white noises. Actually, the computation of the equations of motions in the Euler scheme reads

$$\begin{pmatrix} x_1(t+\Delta t) \\ y_1(t+\Delta t) \\ z_1(t+\Delta t) \\ x_2(t+\Delta t) \\ \cdots \\ \cdots \\ \cdots \end{pmatrix} = \begin{pmatrix} x_1(t) \\ y_1(t) \\ z_1(t) \\ x_2(t) \\ \cdots \\ \cdots \\ \cdots \end{pmatrix} + \Delta t\mathscr{H}\begin{pmatrix} f_1^x(t) \\ f_1^y(t) \\ f_1^z(t) \\ f_2^x(t) \\ \cdots \\ \cdots \\ \cdots \end{pmatrix} + \sqrt{2k_BT\Delta t}\mathscr{A}\begin{pmatrix} \psi_1^x(t) \\ \psi_1^y(t) \\ \psi_1^z(t) \\ \psi_2^x(t) \\ \cdots \\ \cdots \\ \cdots \end{pmatrix} \tag{17}$$

where f_i^β are the forces due to the harmonic springs for the ith bead in the β axis and ψ_i^β are the corresponding components of $\vec{\psi}$.

The computation of $\mathscr{A}$ can be performed exactly by diagonalizing $\mathscr{H}$. This exact diagonalization requires an extremely high computational cost for long chains. The widely used method based on the orthogonal polynomials decomposition (which gives very exact results) is still too slow to get the runs long enough for our purposes. Therefore, we decided for a simple approximate approach based on the perturbation expansion of the hydrodynamic interaction.

To do this we write $\mathscr{H}$ as $\mathscr{I} + r_0\mathscr{S}$, and then expand the square root $\mathscr{A} = \sqrt{\mathscr{I} + r_0\mathscr{S}}$ in powers of r_0

$$\mathscr{A} \approx \mathscr{I} + \frac{r_0\mathscr{S}}{2} - \frac{r_0^2\mathscr{S}^2}{8} + \cdots \tag{18}$$

Since in the thermal equilibrium the averages $\langle E_{tot}\rangle$ being the internal energy and $\langle L^2\rangle$ (also being a thermodynamical quantity following immediately from equipartition) are not modified by the dissipative coupling introduced by the Oseen tensor, we can numerically check the validity of the approximations for $\mathscr{A}$ for different r_0 values. We see that $\langle L^2\rangle$ is extremely sensitive to incorrect incorporation of the hydrodynamic interaction, and its calculation is used as a probe of the quality of the approximation, see Tables 1 and 2. The data for the Rouse model give us typical error bars for the simulation of the exact model on the same scale.

Looking at Tables 1 and 2, one can conclude that for r_0 up to 0.2, the second-order approximation is sufficient, and for r_0 up to 0.1, the first-order approximation (much shorter simulations) is accurate enough. In the case $r_0 = 0.5$, also the second-order approximation is insufficient. Thus, in our simulations we restrict ourselves to $r_0 \leq 0.2$. Once again we stress that such small hydrodynamic radii are rather unrealistic, but they still allow for discussing some qualitative effects of the hydrodynamical interaction.

We use a second-order Runge−Kutta method to solve eq 17 with a sufficiently small time step $\Delta t = 10^{-3}$. For the results shown in this paper we run 2×10^7 iterations up to a maximum time $t = 2 \times 10^4$ for a full trajectory needed for adequate statistics. An initial thermalization period of 1000 time units is performed in all cases in order to start the trajectories from a thermal equilibrium state. The *Compaq AlphaServer HPC320* used to run these simulations requires about 3 h of CPU time for $N = 51$ when the first-order approximation scheme is chosen. The second perturbative order requires more than 120 h of CPU time for the same number of iterations and chain length. In the numerical results shown in this paper, energy is given in units of k_BT, and length in units of $\sqrt{k_BT/k}$. The time scale is determined by the choice $\gamma = 1$.

3. Results

Although the overall role of flow and hydrodynamical interaction is rather clear, the behavior of the intensity as a function of parameters α and r_0 is not trivial. The flow elongates the molecule, so that the typical end-to-end distance grows with α while the hydrodynamical interactions slow the dynamics of intramolecular relative motion, which increases the characteristic time spent in the *on*-state.

The behavior of $I(\lambda)$ as a function of hydrodynamic radius and flow intensity strongly depends on the relation ρ between the reaction radius, a, and the equilibrium end-to-end distance of the polymer (i.e., the one in the absence of the flow), $L = \sqrt{\langle L^2\rangle}$. For $\rho \ll 1$, the polymer is typically in the *on*-state, and thus the

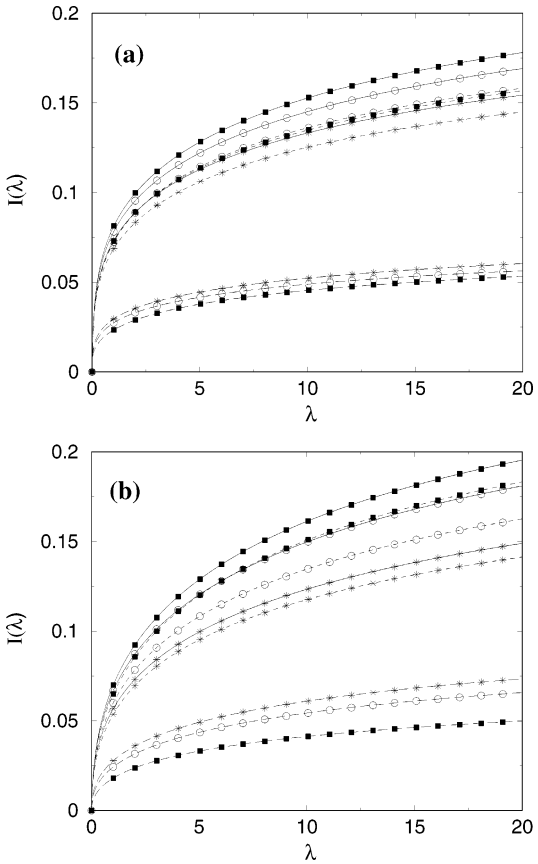

Figure 2. Intensity of steady-state luminescence in the *on*−*off* model as a function of irradiation intensity λ for a reaction radius such that $\rho \ll 1$. In panel a, $N = 21$ and $a = 1$. In panel b, $N = 51$ and $a = 2$. In both panels the same notation is used. The symbol indicates the value of the bead radius: filled squares ($r_0 = 0$), empty circles ($r_0 = 0.05$), and stars ($r_0 = 0.1$), whereas solid, dotted, and dashed lines correspond to $\alpha\tau_R = 0$, 1.05, and 6.56, respectively. $\tau_R = 13.51$ for the chain with 21 beads and $\tau_R = 84.43$ for chains with 51 beads.

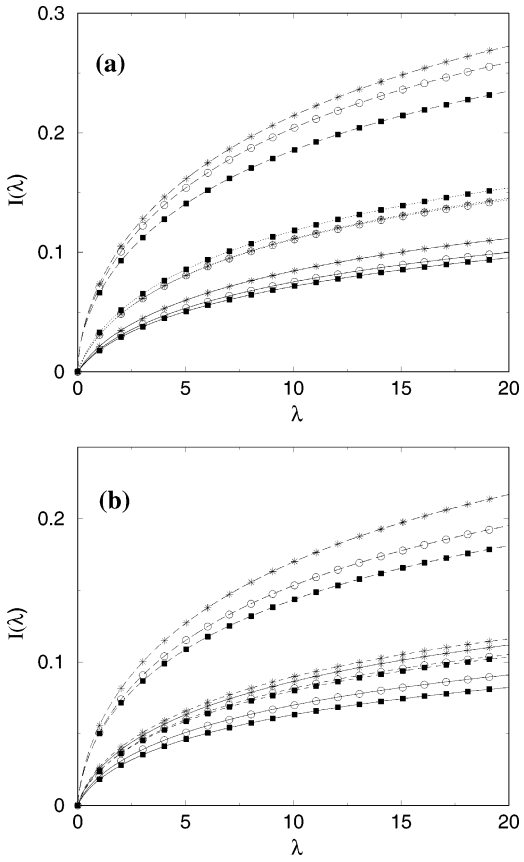

Figure 3. Same as in Figure 2, but now for $\rho \gg 1$. In panel a, $N = 21$ and $a = 8$. In panel b, $N = 51$ and $a = 12$. We use the same notation for the lines as in Figure 2.

flow (elongating the chain and making the transition into the *off*-state less probable) and the hydrodynamic interaction without flow (making the change of states slower) work in the same direction and lead to the decrease in intensity, as is clearly seen in Figure 2.

For $\rho \gg 1$ the molecule is typically in the *off*-state. Increasing flow increases the probability of switching to the *on*-state, and thus leads to increase in the steady-state intensity. The hydrodynamic interaction in the absence of the flow also leads to increasing the typical time in the corresponding state. The effects of the flow and the hydrodynamic interactions for $\rho \gg 1$ are depicted in Figure 3. The increasing effect of the hydrodynamic interaction has to do with the interplay of two factors. On one hand, the longer *on*-intervals get even longer under hydrodynamic interaction, and thus give smaller contributions to the overall intensity. On the other hand, increasing the interaction makes some short *on*-intervals that were not resolved on the time scale λ^{-1} to become longer in such a way that is now resolved on that characteristic minimum time scale, leading to large positive contributions to the overall intensity. As can be concluded from the results in Figure 3, the latter effect increases the intensity with a contribution that surpasses the loss due to the former effect.

This explanation shows that the role of hydrodynamic interaction is rather subtle, and may lead to interesting effects for both regimes ($\rho \ll 1$ and $\rho \gg 1$), especially when the flow is present. Indeed, the effect of hydrodynamic interaction for the cases with $\alpha \neq 0$ depends in a fine way on all parameters, and may act in opposite directions (compare the curves for no flow and high flow, $\alpha\tau_R = 6.56$, in both panels of Figure 2, and the curves for no flow and moderate flow, $\alpha\tau_R = 1.05$, in the upper panel of Figure 3).

The presented results correspond to the model that considers that the donor−acceptor system cannot be excited when being in the *off*-state. The values of P_{off} which are necessary to establish the connection with the situation where the *off*-state can be excited, eq 2, are given in Tables 3 and 4 for $N = 21$ and for $N = 51$, respectively. The intensities of the flows in these tables correspond to the same values of the dimensionless flow intensities $\alpha\tau_R = 0$, 0.176, 1.05, and 6.56 for $N = 21$ and for $N = 51$ chains (the Rouse times being $\tau_R = 13.51$ and $\tau_R = 84.43$, respectively).

4. Conclusions

We presented the results of numerical simulations of the intensity of steady-state luminescence of single polymer chains in a dilute solution due to excitation quenching in a simple model in which donor and acceptor are attached to the ends of the chain. The chain is modeled by simple Rouse dynamics without or with hydrodynamic interactions, which are taken into account in a perturbative manner. We consider the situations of a quiescent solvent as well as the chain in a shear flow. Depending on the relation between the effective distance for energy transfer and the typical end-to-end distance of the chain different regimes are

encountered with respect to dependence of the steady-state luminescence intensity on the strengths of the flow and of interaction. Such luminescent probes may be used for experimental flow diagnostics.

Acknowledgment. The authors acknowledge helpful discussions with H. Kauffmann, J. M. Sancho, and F. Sagués. We thank CESCA (Centre de Supercomputació de Catalunya) for financial and computational support through the "Improving the Human Potential" Program. I.M.S. gratefully acknowledges partial financial support by the Fonds der Chemischen Industrie.

References and Notes

(1) Burlastsky, S. F.; Oshanin, G. S.; Mogutov, A. V. *Phys. Rev. Lett.* **1990**, *65*, 3205; Pálszegi, T.; Sokolov, I. M.; Kauffmann, H. *Macromolecules* **1998**, *31*, 2521; Sokolov, I. M.; Mai, J.; Blumen, A. *J. Lumin.* **1998**, *76*−*77*, 377; Sung, J.; Lee, S. *J. Chem. Phys.* **2001**, *115*, 9050; Srinivas, G.; Sebastian, K. L.; Bagchi, B. *J. Chem. Phys.* **2002**, *116*, 7276.
(2) Wilemski, G.; Fixman, M. *J. Chem. Phys.* **1974**, *60*, 866; *ibid* **1974**, 878.
(3) Doi, M. *Chem. Phys.* **1975**, *9*, 455.
(4) Szabo, A.; Schulten, K.; Schulten, Z. *J. Chem. Phys.* **1980**, *74*, 4350.
(5) de Gennes, P. G. *J. Chem. Phys.* **1982**, *76*, 3316.
(6) Pastor, R. W.; Zwanzig, R.; Szabo, A. *J. Chem. Phys.* **1996**, *105*, 3878.
(7) Bandyopadhyay, T.; Ghosh, S. K. *J. Chem. Phys.* **2002**, *116*, 4366.
(8) Sokolov, I. M. *Phys. Rev. Lett.* **2003**, *90*, 080601.
(9) Fredrickson, G. H.; Leibler, L. *Macromolecules* **1996**, *29*, 2674.
(10) Kolb, A.; Marques, C. M.; Fredrickson, G. H. *Macromol. Theory and Simul.* **1997**, *6*, 169.
(11) Rice, S. O. *Bell Syst. Technol. J.* **1945**, *24*, 51. See also: Cramér, H.; Leadbetter, M. R. *Stationary and Related Stochastic processes*; Wiley: New York, 1968. See also a simple account in: Ziman, J. M. *Models of Disorder: The Theoretical Physics of Homogeneously Disordered Systems*; Cambridge University Press: Cambridge, U.K., 1979.
(12) Eisenberg, R. S.; Klosek, M. M.; Schuss, Z. *J. Chem. Phys.* **1995**, *102*, 1767.
(13) Rouse, P. E. *J. Chem. Phys.* **1953**, *21*, 1272.
(14) Bueche, F. *J. Chem. Phys.* **1954**, *22*, 603.
(15) Fixman, M. *Macromolecules* **1986**, *19*, 1204.
(16) Rzehak, R.; Kienle, D.; Kawakatsu, T.; Zimermann, W. *Europhys. Lett.* **1999**, *46*, 821.
(17) Rzehak, R.; Zimermann, W. *Europhys. Lett.* **2002**, *59*, 779.
(18) Zimm, B. H. *J. Chem. Phys.* **1956**, *24*, 269.
(19) Doi, M.; Edwards, S. F. *The Theory of Polymer Dynamics*; Cornell University Press: Ithaca, NY, 1981.

MA048593B